

Portable Small-Scale Vertical Axis Wind Turbine with Pitch Angle Control System (H-Type VAWT)

Naguib Saleh¹, Adel Kamal², Ahmed Mahmoud³, Ali Moustafa⁴, Hedaya Farid⁵, Pola Osama⁶

¹Doctor, Department of Mechanical Engineering, Canadian International College (CIC), Cairo, Egypt

^{2,3,4,5,6}Students, Department of Mechanical Engineering, Canadian International College (CIC), Cairo, Egypt

Abstract - This Research paper aims to document the process of designing & manufacturing a proof of concept of a portable vertical axis wind turbine with A novel control method is also demonstrated to offer exciting possibilities for improving existing VAWTs. The idea behind the portable design is for the user to be able to take the wind turbine to remote places that lack electrical energy for long periods of time like refugee camps & military barracks, the reason for using the pitch angle control system is that by varying the pitch angle of the blade this generates more lift force on it which corresponds to a higher level of energy absorption and output power.

Key Words: Lift force, Portable, Vertical Axis, Wind turbine, Darrieus vertical axis wind turbine (H-type VAWT), Computational fluid dynamics (CFD), Variable pitch angle control, Control, pitch angle.

1. INTRODUCTION

Energy resources can be divided into two types non-renewable (oil, coal, and natural gas) and renewable (wind, solar, geothermal, and hydropower) [1]. As non-renewable energy resources are becoming scarce and expected to run out shortly [2], therefore it is a fact that ways to obtain energy from renewable resources must be developed to satisfy the current and future needs of power consumption. In this chapter; the types of non-renewable and renewable energy will be discussed to understand the importance of using renewable energy.

1.1 Non-Renewable Energy

Fossil fuels are generated from the preserved remains of plants and animals and are found underground, as their collective name suggests. Fossil fuels include coal, petroleum, natural gas, oil shale, bitumens, tar sands, and heavy oils. All of them contain carbon and are formed due to the geologic process that acts on the remains of organic matter and this process takes 300 to 400 million years to form naturally [3].

All fossil fuels can be burned in the air to produce Thermal energy; this energy can then be used directly like in home furnaces or can be used to heat water which in turn produces steam which drives a turbine to generate electricity, this process is called geothermal power generation [4].

The applications mentioned are essential for a lot of industries. However, fossil fuel combustion does more harm than good due to the large amounts of harmful emissions such as CO₂, Greenhouse gases & particulate Matter which consequently affects not only the environment but also the General well-being of the population [5]. According to the Intergovernmental Panel on Climate Change (IPCC) in 2018, it was calculated that 89% of global CO₂ Emissions came from fossil fuel combustion and that fossil fuel usage is the root cause of global warming [6, 7].

Client Earth and IPCC warn that fossil fuel consumption must be halved in the next 11 years to avoid exceeding a global temperature rise of 1.5°C, which would cause severe consequences such as increased sea levels, extinction to certain species of animals and crops, and extreme weather [6, 7]. However, a report published by the *United Nations Climate Change* reveals that current efforts are insufficient to prevent temperatures from rising above 1.5°C by the end of 2030, and the world may be on track for around 2.5°C of warming by the end of the century. Luckily in the 1980s, the familiar sustainable forms of energy were presented (solar & wind) [8].

This new approach to renewable energy generation is crucial for our survival and as the *International Renewable Energy Agency* (IRENA) Director-General *Francesco La Camera* said "We are staring into a terrifying abyss of irreversible climate consequences if we fail to act," [9].

Moreover, Crude oil reserves are depleting at a rate of more than 4 billion tons a year and at this rate, our known oil reserves could run out in just over 53 years. If we increase gas production to fill the energy gap left by oil, our known gas reserves will also be used up within 52 years. And if people try to accommodate for the decrease in the production of oil and natural gas by coal, the known reserves will be empty after nearly 150 years [2].

1.2 Renewable Energy

Renewable energy resources are the sources that naturally renew themselves at a rate that makes them seem infinite. There are many types of renewable sources of energy such as (solar, wind, hydro, tidal, geothermal, and biomass) [10].

2.0 Mechanical Design

When determining the overall dimension of the project, various factors were carefully considered to ensure the best outcome. One of the most important considerations was portability, as it needed to be easily transported from one location to another. Additionally, the product was designed to cater to smaller-scale operations, making it more accessible to a wider range of users. User-friendliness was also a key consideration, as the goal was to create a product that was easy to use and navigate, even for those with limited technical knowledge. All these factors were carefully weighed and balanced to create a final product that was both functional and user-friendly.

The portable wind turbine can be divided into two main parts upper, and lower limbs. Upper limbs are the links, four bar mechanism, servos, and blades. Lower limbs are the electronic housing, legs, and base which connects the lower and upper parts.

2.1 Upper body of turbine

The blades have an airfoil NACA0018 profile with a chord length of 190mm. Blades change their pitch angle using a servo motor controlled by a microcontroller. Furthermore, the links that hold the blades, are designed to contract and extend using a four-bar mechanism. Designing such mechanism needed to have a smooth transformation between the mentioned two states which encouraged the idea of using the four-bar mechanism with gears as shown in figure 1. However, a Complex mechanism dictates having a part with complex geometry as a complementary. The most complex piece geometrically is the servos' holders, working as an intermediate part between the servo and the blade shown in figure2.

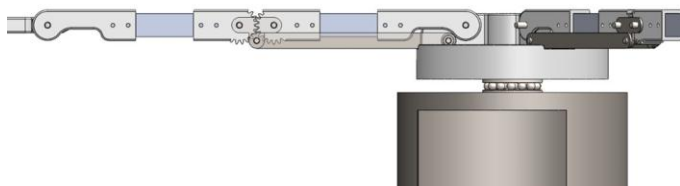


Figure 1: Four-bar mechanism and Gears.

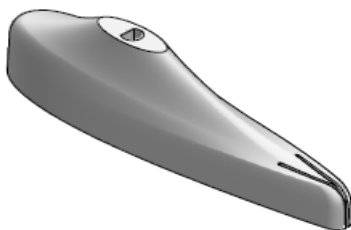


Figure 2: Holder of blades

2.2 Lower body of turbine

The tripod acts as the base of the portable wind turbine, providing the necessary support and stability. The main objective of the design was to create a mechanically robust structure that could withstand the dynamic forces exerted by the wind turbine. The placement of the legs at a 45-degree angle from the base provided a stable and stable platform, reducing the risk of slippage or excessive vibration during work This arrangement these considerations are necessary to maintain the design integrity of the wind turbine under different wind conditions. First, the initial design of the tripod featured three legs positioned at a 45-degree angle from the base, ensuring stability and rigidity against external forces. The tripod comprises three main parts: the base, fixation plate, and legs, as depicted in Figures 3, 4, and 5, respectively.

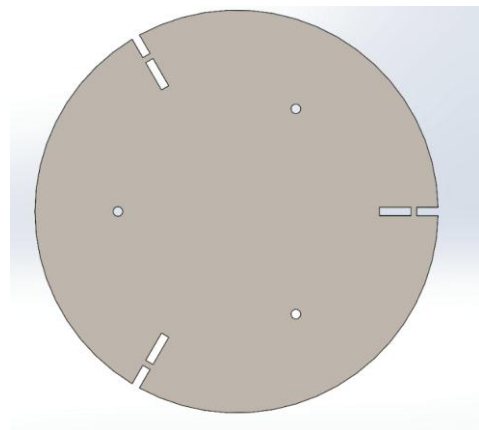


Figure 3: Base

The base is the intermediate part between rotating links and the legs. The Fixation plate is used to connect base and legs. Finally, the legs are used to stabilize the wind turbine using friction produced between legs ends and ground. In figure 4, the tripod is able to shrink in size via moving legs towards the center -closing- by pivoting around the fixation point in the fixation plate. Furthermore, the legs are able to be extended in case of the ground is not flat or had low friction coefficient.

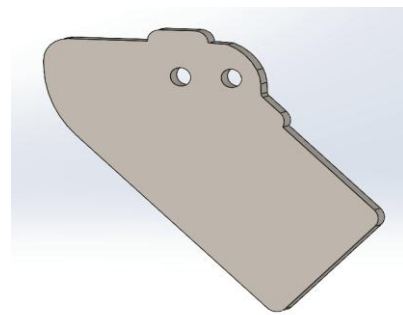


Figure 4: Fixation plate



Figure 5: Tripod closed

Figure 6: Tripod fully extended

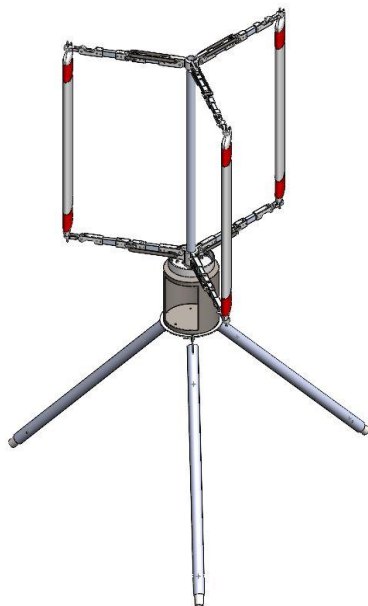


Figure 7: Final Design

3.0 Stress analysis

A stress analysis was conducted on the lower parts of the wind turbine shown in the figure 8. The stress analysis was done using a 100 kg using SolidWorks 2020. Results of this simulation was conclusive that the geometry and material selection of Aluminum was adequate and more than enough. Putting these findings as followed allows to draw a conclusion that the Tri-pod is safe for commercial use.

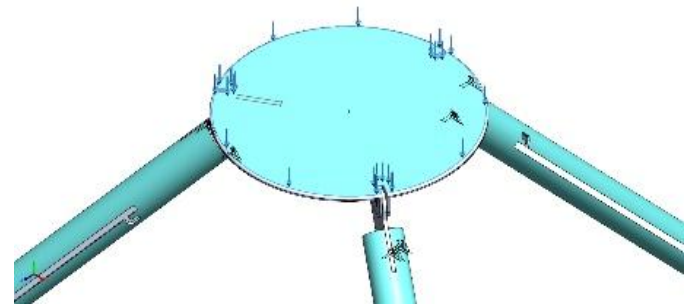


Figure 8: Stress analysis on Tri-pod

4.0 Aerodynamics parameters associated with Vertical Wind Turbine

Tip speed ratio (TSR) (λ), a significant characteristic related to VAWT blades, is calculated with using the following equation,

$$\lambda = \frac{R \times \omega_r}{u_\infty}$$

R is the rotor radius, ω the rotational speed of the rotor, and u_∞ wind velocity [12].

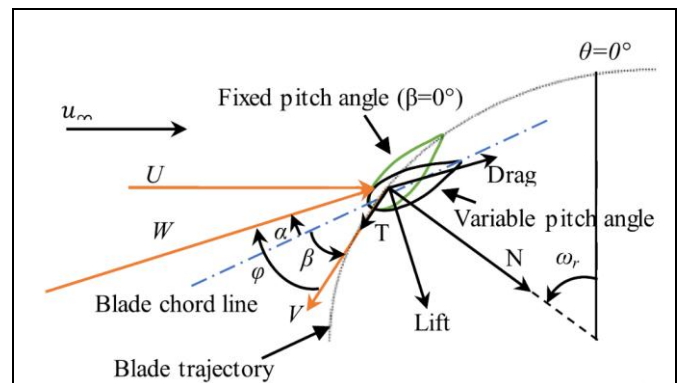


Figure 1: Forces and velocities acting on the blade of a Darrieus turbine [12]

The forces acting on each blade can be used to predict the actual VAWT performance. Figure 28 depicts the Vectors of velocity and force acting on Darrieus turbine blades. The tangential velocity vector of the rotor is represented by the velocity \vec{v} . The relative velocity is represented by the resultant velocity vector \vec{w} , which is composed of the induced velocity (U) and blade velocity (V) vectors. The angle of attack (α) is typically defined as the angle formed by the relative velocity direction, W, and the chord line of the

blade. The pitch angle of the blade is as specified in Ref. [13] where φ is the angle formed by the directions \vec{v} and \vec{w} . The angle of attack (α) and relative wind speed (W), which is a function of the azimuth angle (θ), obviously continuously change during each cycle. As a result, the magnitude and orientation of both the lift and drag forces vary with the azimuthal position of the blade. The main forces acting on VAWT blades are also depicted in Figure 28 lift, drag, normal (N), and tangential (T). The tangential force (T) [13] can be used to estimate rotor performance. The power coefficient (C_p) is the ratio of mechanical power generated by the wind turbine (P_m) to wind power available (P_w) [14].

$$C_p = \frac{P_m}{P_w} = \frac{w_r \tau_r}{\left(\frac{1}{2}\right) \rho A u_\infty^3} = \frac{w_r \left(C_m \times \frac{1}{2} \rho A U_\infty^2 R\right)}{\frac{1}{2} \rho A u_\infty^3} = C_m \frac{\omega_r R}{u_\infty} = C_m \lambda$$

where ρ is the air density (1.225 kg/m³), and A is the area swept by the turbine (e.g., for the H-type Darrieus wind turbine, $A = 2RH$, where H is the blade length). However, for VAWTs at low TSRs, a negative torque is often generated because of the large dynamic cyclic variations in the angle of attack (α).

5.0 COMPUTATIONAL FLUID DYNAMICS (CFD)

5.1 Introduction

Studying the characteristics of wind turbines was expensive due to the use of wind tunnels. The rise of more powerful computers had given researchers a new tool to study the behavior of almost any system when in contact with dynamic fluid loads. Inexpensive and comprehensive as it is, this method was favorable to be used for a graduation project. The goal of studying wind turbine behavior is to determine best way of increasing performance by using a control system for pitch angle of each blade.

5.2 The CFD model

Ansys fluent was used because it has intuitive interface and free license for students. Simulation was a 2-D three-bladed H-Darrieus VAWT with NACA 0018 airfoil at different tip speed ratios for both fixed and variable pitch angle configurations. Sliding mesh technique was appropriate as the desired measured outputs were variable in time which required the use of a transient simulation.

| FEATURE | VALUE |
|--------------------------------|---------------------|
| ROTOR RADIUS (R) [MM] | 656 |
| BLADE HEIGHT (H) (2D) [MM] | 1000 |
| BLADES NUMBER (NB) [-] | 3 |
| BLADE PROFILE [-] | NACA 0018 |
| CHORD @ [MM] | 190 |
| PITCH ANGLE (B) [°] | -6,-4,-0,4,6 |
| AZIMUTH ANGLE (Θ) [°] | 0 to 360 |
| TIP SPEED RATIO (λ OR TSR) [-] | 1, 1.7, 2, 2.7, 3.3 |

5.3 Ansys Pre-process

CFD simulations with Ansys are not magically done. First upload the required geometry. Second apply a good mesh on top of it. Third tune the parameters of the simulation. All explained in the following section.

A. Geometry:

The geometry is divided into multiple domains as follow:

1. Stationary domain: The dimensions need to large enough to prevent a solid blockage effect of the lateral boundaries Therefore, the dimensions of the domain are 40 rotor diameters upstream (L1), 100 rotor diameters downstream (L2), and 60 rotor diameters width (W) [11].

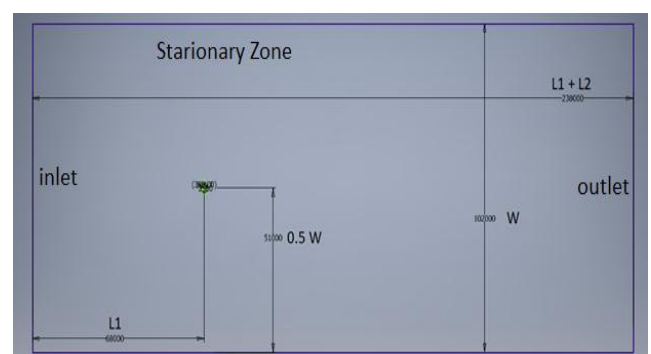


Figure 10: Stationary Domain

2. Rotating domain: Usually it's recommended to use as small as it could be to better describe the vorticity accurately and avoid undesirable disturbances generated at the interface. The radius was found to be approximately 2.95 of the rotor's radius.

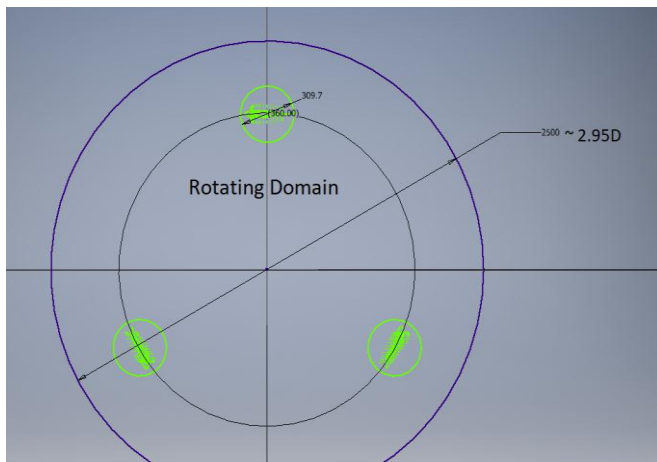


Figure 11: Rotating Domain

- Blade sub-domain: Additional circular sub domains are added to have a finer mesh around the airfoils. Airfoils are hard to study because of its fast and highly changeable pressure around it with every step. The radius of the domain was approximately 1.6 the length of blades' chord.

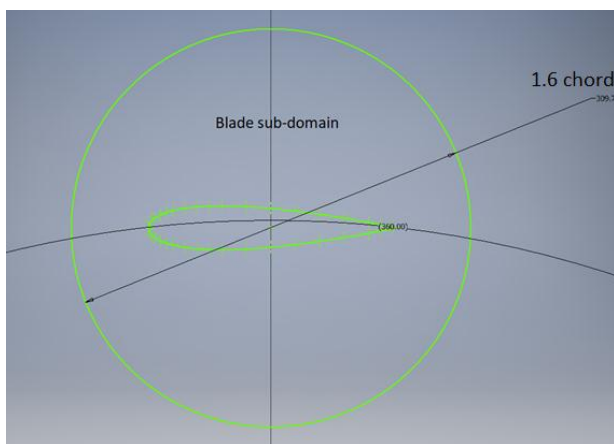


Figure 12: Sub-Domain

B. Generating mesh

Generating mesh is relatively hard process as it decides complexity degree of solving the simulation. Although a complex simulation to solve is desired for its accurate results, the downside is the need of better technology and patience, which means more money, to solve these hard problems. The core problem is now clear, when generating mesh, engineers should balance between accuracy and cost.

According to the literature [11], the biggest two factors affecting this kind of CFD is the value of Y^+ and Courant-Friedrichs-Lewy number (cfl) within a distance of 10 mm far from the blades and at the interface of rotating zone. The element size on the interface of rotating zone has been set to 39 mm.

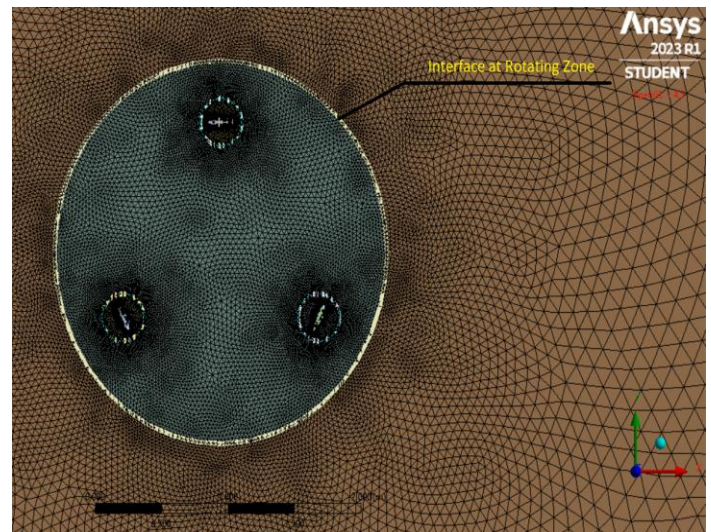


Figure 13: whole Turbine after applying modification on mesh

The solver is quite capable at capturing the pressure and shear stress in elements when it's in the viscous sublayer or fully turbulent sublayer. concluding to have elements close to the wall to have Y^+ close or under one [11] to ensure accurate results. The blade was set to have 525 nodes on edge and an inflation for 30 layers with first element thickness of $1e-5$ ensuring a Y^+ under 1.

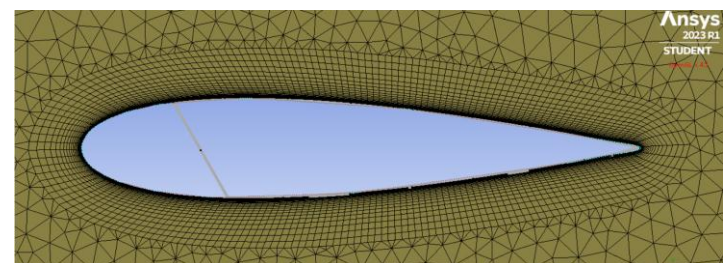


Figure 14: Blade after applying inflation on its edge

C. Fluent solver

ANSYS-Fluent uses many turbulence models based on Reynolds-averaged Navier-Stokes (RANS) equations to represent the turbulent properties of the flow. These models typically include two additional transport equations that are solved for the turbulence kinetic energy (k) and its dissipation rate (ϵ or ω). The Shear-Stress Transport (SST $k-\omega$) model has been used when the literature was revised [11].

5.4 Results:



Figure 15: Coefficient of performance of portable wind turbine under normal operation.

6.0 Control:

In fixed angles lift is created by only 1 or 2 blades that are meeting the wind flow at a better angle then slowed by a breaking turbulence generated from the remaining blades meeting the air at a worse angle. So, this makes other blades suffer from mixed-up (vortex) air causing limited output from available wind energy.

Therefore, variable pitch system shows lift from more than two blades and less drag from others. Which translates into a higher level of wind energy absorption and output in the form of power or mechanical drive energy solving the main issue of vertical wind turbines making it self-starting.

First, The Anemometer that is placed beside portable wind turbine measures Wind speed (V_W) and pass value to the micro-controller. Then, The Incremental Encoder mounted on the rotor shaft sends logical signals to micro-controller for determining position and rotational velocity of rotor shaft. The micro-controller uses previous mentioned values to calculate Tip speed ratio (TSR). Select the best pitch angel (β) according to the best coefficient of performance C_P to the current TSR at the end of the cycle each servo motor - attached to each blade- will receive the suitable pitch angel in respect of the blade's position -Azimuth angel (θ). A simple schematic figure 33 represents what was mentioned up-close to further clarification.

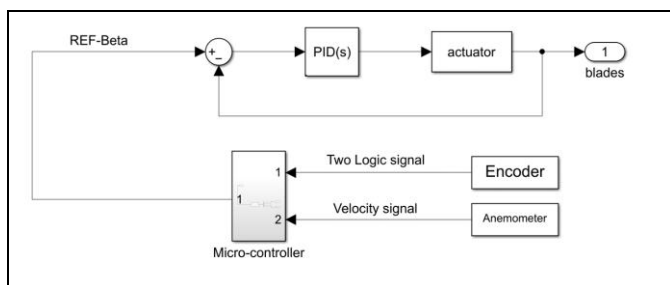


Figure 16: Schematic of control

7.0 Cost Analysis

This analysis was carried out according to the Egyptian prices in June 2023.

As startup company manufacturing 25 wind turbine per month:

one-time fixed cost (FC_{OT}):

Machines cost= (2 x 3d printer) + (1 x laser metal cutting machine) + (1 x laser wood cutting machine) + (1 x arc welding) = (2 x 20,000) + (1x15,000) + (1x120,000) + (1x5,000) = 160,000 EGP

Fixed cost per month (FC_M):

Employee's cost:

(2 workers x 3,000) + (1 Maintenance worker x 3,500) + (2 engineers x 8,000) + (10,000 renting cost) = 35,500 EGP/month.

Power consumption of the facility per month:

Electricity cost: (1000 Kwh/month) x (1.45 EGP/Kwh) = 1,450 EGP/month

Total fixed cost per month (FC_M) = (35,500) + (1,450) = 36,950 EGP

Variable cost:

Variable Cost per unit (v):

Material used for one wind turbine:

MDF wood (50) + Balsa Wood (1,100) + beech wood (100) + bearings (240) + bolts and nuts (200) + Abs filaments (5,000) + aluminum Links 3kg (1,500) + aluminum sheets 1kg (500) + aluminum pipes 8kg (5,000) + aluminum shaft 2kg (1,000) = 14,690 EGP

Electronics Components:

servo motors x3 (1,500) + wires (100) + Alternator (17,000) + 2 batteries (1,500) + slip ring (800) + Arduino UNO (760) + inverter (1,000) + Bluetooth module x2 (400) + breadboards (50) + regulator (300) + anemometer (1,200) + encoder (750) = 25360 EGP

Variable Cost per unit (v) = 14,690 + 25360 = 40,050 EGP

According to the revenue per unit (r) is 46,000 EGP therefore:

Profit per unit = revenue per unit - variable cost per unit = 46,000 - 40,050 = 5950 EGP

8.0 CONCLUSION

In conclusion, the findings from the real-time Internet of Things (IoT) data and MATLAB analysis provide valuable insights into the impact of blade pitching on the performance of wind turbines. The results demonstrate that employing positive pitch angles can significantly enhance the power coefficient at low Tip-Speed Ratio (TSR) of 1, resulting in an approximate 4% increase in Cp.

By comparing the power coefficient values, which increased from 0.03815712 to 0.041201, it is evident that the blade pitching approach has a positive effect on the turbine's performance. This improvement indicates that the wind turbine's self-starting capabilities can be enhanced, allowing

it to reach its nominal operating speed without the need for additional power.

These findings have important implications for the field of wind energy, as they suggest that optimizing blade pitching can contribute to more efficient and cost-effective wind turbine operations. By utilizing the blade pitching approach, wind turbine systems can harness a higher proportion of the available wind energy, maximizing power generation potential.

REFERENCES:

1. Energy.gov. *Energy Sources*. 2022; Available from: <https://www.energy.gov/energy-sources#:~:text=Primary%20energy%20sources%20take%20many.%2C%20solar%2C%20geothermal%20and%20hydropower>.
2. Kalair, A., et al., *Role of energy storage systems in energy transition from fossil fuels to renewables*. *Energy Storage*, 2021. 3(1): p. e135.
3. Kopp, O.C., *Fossil Fuel*. *Encyclopedia Britannica*, 2022, December 16.
4. Curley, R., *Fossil fuels*. 2011: Britannica Educational Publishing.
5. Osman, A.I., et al., *Cost, environmental impact, and resilience of renewable energy under a changing climate: a review*. *Environmental Chemistry Letters*, 2022.
6. Client Earth. *Fossil fuels and climate change: the facts*. 2022, February 18; Available from: <https://www.clientearth.org/latest/latest-updates/stories/fossil-fuels-and-climate-change-the-facts/#:~:text=When%20fossil%20fuels%20are%20burned,temperature%20has%20increased%20by%201C>.
7. Masson-Delmotte, V., et al., *Global Warming of 1.5° C: IPCC Special Report on Impacts of Global Warming of 1.5° C above Pre-industrial Levels in Context of Strengthening Response to Climate Change, Sustainable Development, and Efforts to Eradicate Poverty*. 2022: Cambridge University Press.
8. United Nations Climate Change. *Climate Plans Remain Insufficient: More Ambitious Action Needed Now*. 2022, October 26; Available from: https://unfccc.int/news/climate-plans-remain-insufficient-more-ambitious-action-needed-now?utm_campaign=The%20Batch&utm_medium=email&hsmi=232282177&hsenc=p2ANqtz--zkt5jX6GQ5lao_HMrt4K3FIwCpi201mPerybWR1cXZ8zLRHc7ot8kVX8-Q7EiIv17f6M4e7MnXetnDsyKYVjdIYBwA5Rgbl2T-lbxRDY27NflgQ&utm_content=232281151&utm_source=hs_email.
9. International Renewable Energy Agency. *We face an abyss of irreversible climate consequences, says IRENA DG*. 2022, October 27; Available from: <https://www.irena.org/News/pressreleases/2022/Oct/We-face-abyss-of-irreversible-climate-consequences-says-IRENA-DG#:~:text=%E2%80%9CWe%20are%20staring%20into%20a,Director%2DGeneral%20Francesco%20La%20Camera>.
10. Johns Hopkins. *Renewable Energy vs Sustainable Energy: What's the Difference?* 2021, July 2; Available from: <https://energy.sais.jhu.edu/articles/renewable-energy-vs-sustainable-energy/>.
11. Kumar, R., K. Raahemifar, and A.S. Fung, A critical review of vertical axis wind turbines for urban applications. *Renewable and Sustainable Energy Reviews*, 2018. 89: p. 281-291.
12. Abdalrahman, G., W. Melek, and F.-S. Lien, *Pitch angle control for a small-scale Darrieus vertical axis wind turbine with straight blades (H-Type VAWT)*. *Renewable energy*, 2017. 114: p. 1353-1362.
13. Dyachuk, E., et al., *Measurements of the aerodynamic normal forces on a 12-kW straight-bladed vertical axis wind turbine*. *Energies*, 2015. 8(8): p. 8482-8496.
14. Gosselin, R., G. Dumas, and M. Boudreau, *Parametric study of H-Darrieus vertical-axis turbines using CFD simulations*. *Journal of Renewable and Sustainable Energy*, 2016. 8(5): p. 053301.